

Piezoelectric Wafer Stage Based on Highly Variable Viscoelastic Stiffness

Citation for published version (APA):

de Bruijn, R. G. C., Vermeulen, J. P. M. B., & van de Wijdeven, J. J. M. (2023). Piezoelectric Wafer Stage Based on Highly Variable Viscoelastic Stiffness. In *ASPE 2023 Annual Meeting: 38th Annual Meeting of the American Society for Precision Engineering, ASPE 2023, Boston, 12- 17 November 2023* (pp. 1-6). American Society of Precision Engineering (ASPE).

Document status and date:

Published: 15/11/2023

Document Version:

Author's version before peer-review

Please check the document version of this publication:

- A submitted manuscript is the version of the article upon submission and before peer-review. There can be important differences between the submitted version and the official published version of record. People interested in the research are advised to contact the author for the final version of the publication, or visit the DOI to the publisher's website.
- The final author version and the galley proof are versions of the publication after peer review.
- The final published version features the final layout of the paper including the volume, issue and page numbers.

[Link to publication](#)

General rights

Copyright and moral rights for the publications made accessible in the public portal are retained by the authors and/or other copyright owners and it is a condition of accessing publications that users recognise and abide by the legal requirements associated with these rights.

- Users may download and print one copy of any publication from the public portal for the purpose of private study or research.
- You may not further distribute the material or use it for any profit-making activity or commercial gain
- You may freely distribute the URL identifying the publication in the public portal.

If the publication is distributed under the terms of Article 25fa of the Dutch Copyright Act, indicated by the "Taverne" license above, please follow below link for the End User Agreement:

www.tue.nl/taverne

Take down policy

If you believe that this document breaches copyright please contact us at:

openaccess@tue.nl

providing details and we will investigate your claim.

PIEZOELECTRIC WAFER STAGE BASED ON HIGHLY VARIABLE VISCOELASTIC STIFFNESS

R.G.C. de Bruijn¹, J.J.M. van de Wijdeven², and J.P.M.B. Vermeulen^{1,2}

¹Control Systems Technology Group

Eindhoven University of Technology

Eindhoven, The Netherlands

²ASML

Veldhoven, The Netherlands

INTRODUCTION

In the semiconductor industry, complex machines are used for the manufacturing and inspection of Integrated Circuits (ICs). Technology innovation, such as Artificial Intelligence, continue to require further shrink in critical feature sizes of ICs, extending Moore's Law [1] for at least another decade. This results in further enhanced requirements regarding positioning accuracy of stages both in lithography and inspection systems.

Motion profiles of wafer stages differ amongst the various applications. In some cases, the wafer stage stands still during the lithography process or during wafer inspection or metrology. In other cases, the wafer stage is moving at a constant velocity. During exposure or image intake (sub)nanometer accurate positioning is required. When the process is finished, the wafer stage needs to make a fast point-to-point movement or reverse velocity, to move to the next field (location for next exposure or image intake). This movement requires high acceleration to minimize non-productive (overhead) time and increase throughput. As no exposure or image intake occurs during acceleration, less accurate movement is required in this phase.

For moving the wafer stage over a large range with (sub)nanometer accuracy at Point of Interest (PoI), a dual stage architecture is used both in lithography, and inspection and metrology systems. Here, a Short Stroke (SS) fine positioning stage is stacked on top of a Long Stroke (LoS) stage for large course movement to maximize the dynamic range (see Figure 1) [2].

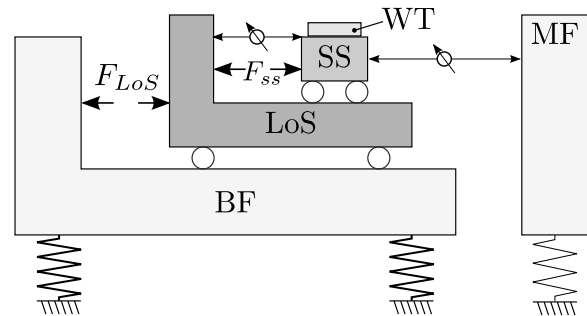


FIGURE 1. Schematic representation of a dual stage concept including: Base Frame (BF), Long Stroke (LoS) stage, Short Stroke (SS) stage, Metrology Frame (MF) and LoS and SS actuators. The Wafer Table (WT) can be considered to be part of the SS.

Lorentz actuators are typically used to achieve high positioning accuracy in SS stages. Using these force actuators (with low position dependency) allows for favorably decoupling of the SS from vibrations originating from the LoS stage, i.e., creates a low disturbance transmissibility. Lorentz actuators, however, have limitations, viz.: low force density, high power dissipation and generation of electromagnetic fields. For Electron beam (E-beam) metrology systems, particularly the latter is highly disadvantageous due to interference of the electromagnetic fields with the electron beams. This poses serious challenges to the stage architecture.

Compared to Lorentz actuators, piezoelectric actuators have a high force density, low power dissipation, and do not generate electromagnetic fields. These actuators, however, are not widely used in semiconductor industry for highly dynamic applications. Namely, the downside of piezoelectric actuators is the high intrinsic mechanical stiffness, which yields an undesirable high disturbance transmissibility [3]. Vibrational motions of the accelerating LoS stage would

result in nearly direct excitation of the SS stage at micrometer level. The high intrinsic mechanical stiffness, however, also has an advantage. It implies very energy efficient actuation of the SS stage by the LoS actuators, with hardly any additional dissipation in the SS actuators. This limited thermal dissipation makes piezoelectric actuators potentially interesting also for lithography applications (multiple kW of dissipation reduction).

To take advantage of the high piezoelectric actuator stiffness during acceleration while minimizing the transmissibility during exposure or image intake, two viable research directions are being investigated: (i) advanced model-based control [4] and (ii) mechanically switching between high to low stiffness during the (short) transition between the acceleration or deceleration phase and the standstill or constant velocity phase.

In this paper, we focus on the concept of mechanically switching between high and low stiffness. Various variable stiffness options have been considered [5]. Creating a variable stiffness using a viscoelastic material looks promising, and is currently subject to further study [6]. Due to the large Poisson ratio, rubbery viscoelastic (RVE) materials are volumetrically nearly incompressible, which means that it has a high resistance against volumetric deformation. By imposing axial or volumetric loading conditions, the stiffness of this RVE material can be changed by multiple orders of magnitude. This will be discussed in more detail later in this work.

MECHATRONIC ARCHITECTURE OF A PIEZOELECTRIC WAFER STAGE

In [5] a new wafer stage mechatronic architecture with variable stiffness is proposed. This architecture takes advantage of the efficient force transfer from the LoS actuators to the Pol at the Wafer Table (WT) during acceleration, and minimizes the transmissibility during standstill or constant velocity. This wafer stage architecture consists of a LoS stage, a Variable Stiffness Device (VSD) an internal balance mass, called Intermediate Body (IB), Piezoelectric SS actuators (PSA) and a Wafer table (WT), as shown in Figure 2.

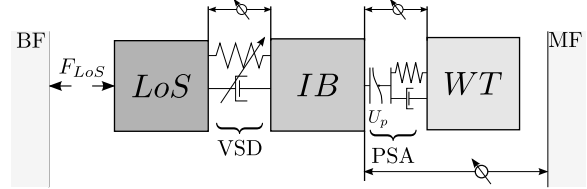


FIGURE 2. *One Degree of Freedom (DoF) model of new mechatronic architecture which includes: a Long Stroke (LoS) stage, Intermediate Body (IB), Wafer Table (WT), Long stroke actuators, Variable Stiffness Device (VSD) and Piezoelectric Short Stroke Actuators (PSA).*

Figure 3 shows the Frequency Response Function (FRF) from LoS position (X_{LoS}) to WT position (X_{WT}) of this mechatronic architecture. In case of a Lorentz actuated SS wafer stage, a very low stiffness level is present between LoS and SS stage, resulting in a very low decoupling frequency of the SS stage followed by a -2 slope ($|X_{WT}/X_{LoS}| \propto 1/f^2$). This slope is advantageous for disturbance isolation but results in inefficient force transfer from LoS to Pol at the WT: If the LoS actuator moves the LoS stage then the SS stage hardly moves. This means that the SS Lorentz actuators also need to generate a force to move the SS stage. Hence, the SS stage acceleration force is generated twice (one time by the LoS actuators and one time by the SS actuators) resulting in significant heat dissipation. For the proposed piezoelectric stage concept, the active SS force is almost neglectable because 1) the VSD between LoS and IB is stiff and 2) the PSA is intrinsically stiff during the acceleration phase. In this acceleration phase the system behaves almost as a rigid body ($|X_{WT}/X_{LoS}| \approx 1$) up to 700 Hz. Above the internal resonance frequency the combined IB and WT mass is decoupled from the LoS mass. This rigid body behavior up to 700 Hz implies a synchronous motion of the LoS stage and WT, with only a small difference in position between the LoS stage and WT as a result of the finite VSD and PSA stiffness. Just prior to the constant velocity or standstill phase in the settling time of a few ms, the VSD is switched to low stiffness resulting in similarly low disturbance transmissibility as compared to Lorentz SS actuators. The transmissibility is slightly higher compared to the Lorentz system because the mass of the moving bodies (IB and WT) is lower than the Lorentz SS stage, targeting a more lightweight stage.

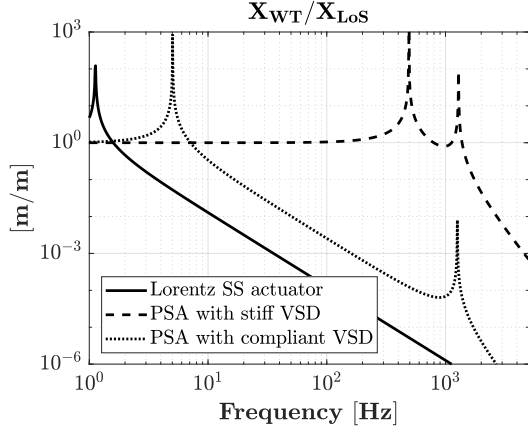


FIGURE 3. FRF from LoS stage position (X_{LoS}) to WT position (X_{WT}) shows the favorable low transmissibility of Lorentz actuators and PSA with compliant VSD.

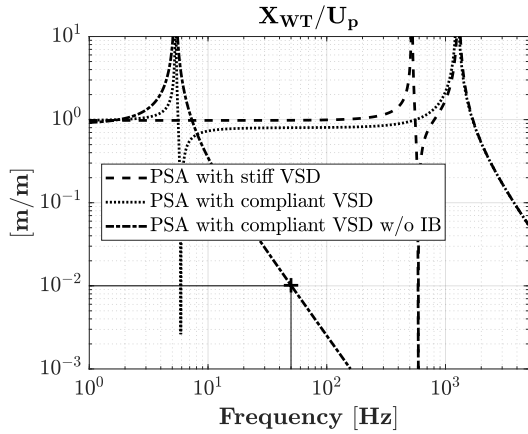


FIGURE 4. FRF from PSA displacement (U_p) to WT position (X_{WT}) shows the working principle of the IB that functions as internal balance mass (right).

Since the IB is decoupled from LoS after acceleration, it serves as an internal balance mass for the PSA. In Figure 4, the FRF from PSA displacement (U_p) to WT (Pol) displacement (X_{WT}) is shown. For the system without IB, just placing the VSD in series with the PSA, the PSA is predominantly compressing the low stiffness VSD rather than actively positioning the WT (dash-dotted line in Figure 4). To move the WT by $1 \mu\text{m}$ at 50 Hz, $100 \mu\text{m}$ actuator displacement would be required. This does not provide a practical solution given the limited stroke of a piezoelectric actuator of about 0.1% of the actuator length. With the IB implemented and a mass ratio m_{IB}/m_{WT} of around 4, the PSA stroke is effectively used to move the WT (amplitude in FRF is 0.8).

VARIABLE STIFFNESS DEVICE (VSD)

The VSD is designed to allow for a stiffness ratio of $c_{high}/c_{low} = 1e4$. A Rubbery Viscoelastic (RVE) material is proposed [6], for the favorable property of being volumetrically nearly incompressible. An indicator for incompressibility is the Poisson's ratio (ν) which is defined as the strain perpendicular to the loading direction divided by the strain in loading direction and is 0.5 for volumetric incompressible materials. For the targeted RVE materials, the Poisson's ratio is between 0.495 and 0.499.

Rubbery viscoelastic materials typically have a low Young's modulus $< 30 \text{MPa}$ [7]. For an RVE material with free expansion capability in lateral direction, Figure 5a, the Young's modulus (E) is felt. In contrast, for the material, which is constrained in lateral direction, Figure 5b the so-called constrained modulus (M) is felt. By changing the loading condition via a preloading, it is possible to vary between a low (E) and high (M) stiffness.

For a Poisson's ratio of 0.499, Equation 3 results in a stiffness ratio $M/E \approx 167$. Equation 4 shows that the theoretical ratio approaches infinity for a Poisson's ratio reaching 0.5.

$$\frac{M}{E} = \frac{1 - \nu}{(1 + \nu)(1 - 2\nu)} \quad (3)$$

$$\lim_{\nu \rightarrow 0.5} \frac{1 - \nu}{(1 + \nu)(1 - 2\nu)} = \infty \Rightarrow M \gg E \quad (4)$$

The axial stiffness for unconstrained axial loading (c_E) and constrained loading (c_M) for a cylindrical shape (see Figure 5a and b) are

$$c_E = \frac{EA}{L} \quad \text{and} \quad c_M = \frac{MA}{L} \quad (5)$$

As a stiffness ratio of $1e4$ is targeted, only changing the loading conditions is insufficient. To further increase the stiffness ratio, the geometry of the RVE material is changed from a cylindrical shape to a conical shape, see Figure 5c and d. For the conical shape at constrained loading condition, a significant part of the force has a short force path through the RVE material and travels mainly through the constraining metal boundary cup. Combining both effects, i.e., change from unconstrained to constrained loading condition and geometrically shorten the force path through the RVE material by the metal

cup, results in a theoretically stiffness increase of about $1e4$ [6].

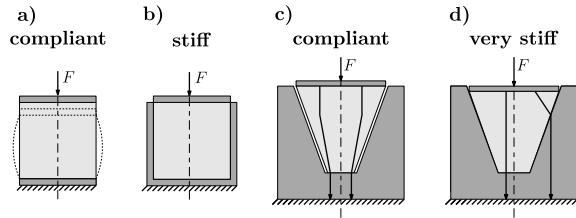


FIGURE 5. Left two figures: Conventional cylindrical shape made out of RVE material, loaded in axial direction without constraining boundaries (a) and with constraint boundaries (b). Right two figures: Conical shape made of RVE both unconstrained (c) and constrained in a metal cup (d), which enable a further increase in stiffness.

Figure 6 shows experimental results of the stiffness increase of a conical RVE material. The stiffness increase is lower than theoretically estimated because of the sub-optimal cone geometry and RVE Poisson's ratio.

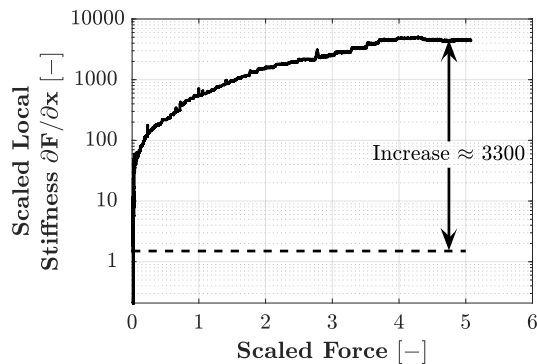


FIGURE 6. Experimental results of stiffness increase of the VSD.

To implement this VSD, two RVE cones and cups are mounted opposite to each other, because the stiffening effect only takes place during compression, and acceleration is in two directions, [6]. To compress the RVE cone in the metal cup two options are considered: a passive and an active configuration (see Figure 7). In the passive configuration, the joint inertia of the IB and WT are used to compress the cone in the cup. Here, the stiffness increase is limited by the force increase from the setpoint (acceleration). This passive configuration results in a significant position error of the WT. This error is too large for the limited stroke of the PSA (see Figure 8).

In the active configuration of Figure 7b two additional piezoelectric actuators are used to press the cones in the cups. The stiffness in the active configuration can be tuned based on the elongation of the piezoelectric actuators and is independent of the motion setpoint both in terms of force and timing. During the stiffness transition, VSD symmetry avoids relative motion between LoS and IB. In addition, since two cones are compressed in parallel the stiffness is doubled compared to the passive configuration. This design, however, comes at the cost of additional piezoelectric actuators. The resulting settling behavior (open loop, i.e., without a WT positioning control loop) of the passive and active concept is visualized in Figure 8.

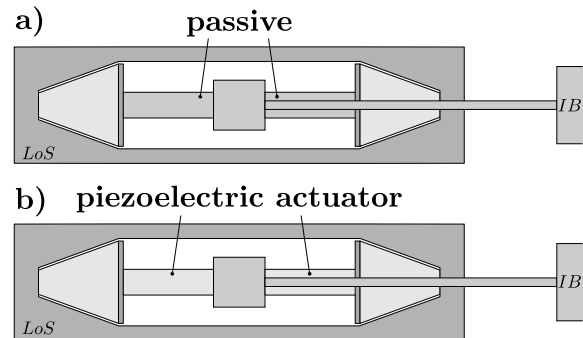


FIGURE 7. Passive configuration of VSD (top) and active configuration of VSD (bottom).

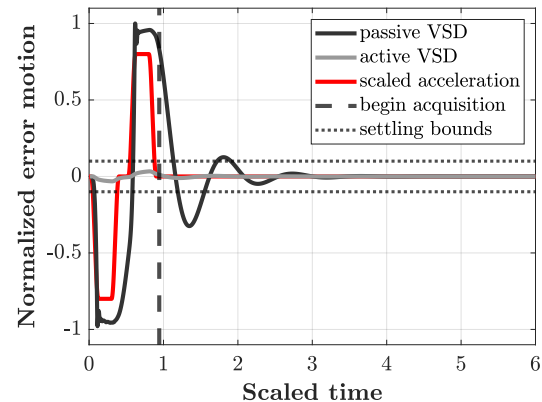


FIGURE 8. Settling behavior of the passive and active VSD configuration (without a controller). For the former the position error is too large for the small PSA stroke to compensate.

SERVO CONTROL

Classical Lorentz-actuated dual stage wafer stages are controlled in primary-secondary configuration [2]. In this configuration, the SS controller accurately tracks the setpoint motion. The LoS controller typically yields less position

accuracy due to limiting dynamics. Its main task is to make sure that the SS actuator stays in its limited actuator range. In the piezoelectric stage configuration, different control strategies are being explored. The challenge in this configuration lies in the highly varying dynamics. In Figure 4 a resonance mode in the SS actuation direction (X_{WT}/U_p) is moving from about 700 Hz to about 7 Hz during the transition from stiff to compliant VSD..

For the piezoelectric actuated wafer stage an alternative control concept is proposed. A LoS controller is used to track the setpoint as accurate as possible (micrometer level) synchronous with VSD switching from stiff to compliant, a SS controller is activated to guarantee accurate motion (nanometer level) during exposure or image intake, as visualized in Figure 9.

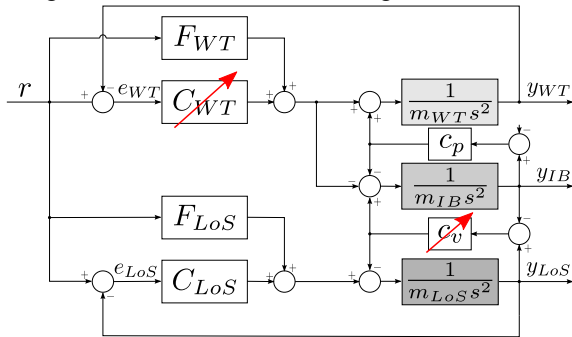


FIGURE 9. Control scheme for the piezoelectric stage with: VSD stiffness (c_v), PSA stiffness (c_p), masses of LoS, IB and WT (m), LoS and WT feedforward controllers (F_{LoS} and F_{WT}), LoS feedback controller (C_{LoS}) and switching feedback controller C_{WT} .

From first analyses, it appears that the servo error of the piezoelectric system with VSD is comparable to the servo error of the Lorentz system during exposure or image intake (see Figure 10).

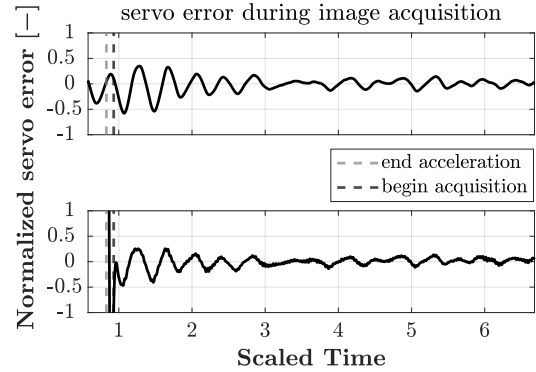


FIGURE 10. Similar behavior during exposure or image intake for 1 DoF model of traditional Lorentz system with linear controllers in primary-secondary configuration (top), and piezo-electric stage with VSD and switching controllers (bottom).

EXPERIMENTAL TEST SETUP

As a next step, a test setup is realized to experimentally validate the concept (see Figure 11). Both the long stroke and intermediate stage are provided with vacuum preloaded air bearings, calibrated Lorentz actuators relative to a force frame and position encoders relative to a separate metrology frame. Between these two stages, the piezoelectric stage will be mounted. This piezoelectric stage demonstrator is currently under construction (see Figure 12).

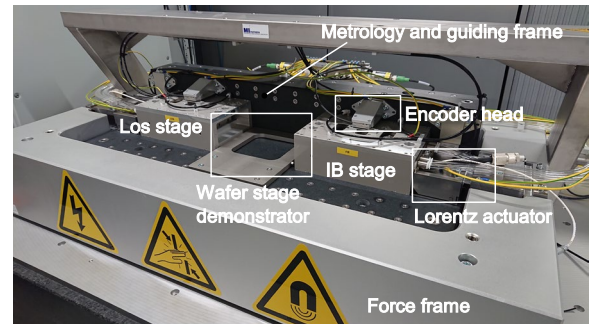


FIGURE 11. Test setup to validate the concept in One Degree of Freedom.

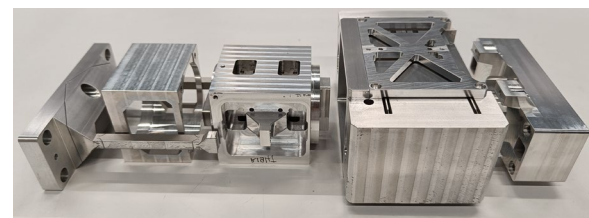


FIGURE 12. Piezoelectric wafer stage demonstrator currently under construction.

CONCLUDING REMARKS

A promising concept is being explored for implementing piezoelectric Short Stroke (SS) actuators as an alternative for Lorentz actuators in lithography and inspection systems for semiconductor industry. Piezoelectric actuators benefit a high force density, low power dissipation and the absence of electromagnetic fields, the latter being highly advantageous for inspection systems. Piezoelectric actuators however, have high intrinsic stiffness which results in high disturbance transmissibility from the Long Stroke (LoS) stage to the Point of interest (PoI) at the wafer table (WT) during exposure or image intake, which highly limits positioning performance. In contrast, a benefit of this high intrinsic stiffness is the energy efficient force transfer from the LoS actuators to WT during acceleration phase of the wafer stage with very little power dissipation.

To take advantage of the high piezoelectric actuator stiffness during acceleration while minimizing disturbance transmissibility during standstill or constant velocity, a variable stiffness device (VSD) based on Rubbery Viscoelastic (RVE) material is proposed. By switching from an unconstrained to a constrained state in a conical shape, a factor of $1e4$ in stiffness variation is targeted. In preliminary experiments at a sub-optimal cone geometry and Poisson's ratio, a factor of $3.3e3$ has been demonstrated. In further research, more advanced shapes of RVE materials are being explored to obtain a higher stiffness ratio and to minimize the effect on lifetime.

An active and passive configuration of the VSD are considered. The active configuration is selected since it allows for higher stiffness and switching independent of the stage motion setpoint, resulting in lower error motion. Downside is that it requires additional piezoelectric actuators.

Motion control for the piezoelectric wafer stage has diverged from the classical primary-secondary configuration as typically used in dual-stage electromagnetic configurations. For this piezoelectric concept, different control strategies are being explored. A promising strategy is to switch controllers synchronized with VSD switching. From analysis it appears that for this configuration, a similar settling performance can be achieved as a Lorentz system. Next step is to experimentally validate the complete mechatronic architecture in one Degree of Freedom.

ACKNOWLEDGMENT

This work is part of the TU/e-ASML mini-Impulse program "Advanced piezoelectric wafer stage for lithography and metrology" partially funded by TKI (TKI-HTSM/17.1429).

REFERENCES

- [1] G. E. Moore, "Cramming more components onto integrated circuits With unit cost," *Electronics*, vol. 38, no. 8, 1965.
- [2] H. Butler, "Position Control in Lithographic Equipment [Applications of Control]," *IEEE Control Syst.*, vol. 31, no. 5, pp. 28–47, Oct. 2011, doi: 10.1109/MCS.2011.941882.
- [3] R. Munnig Schmidt, G. Schitter, A. Rankers, and J. van Eijk, *The Design of High Performance Mechatronics*, 3rd ed. Amsterdam: IOS Press, 2020.
- [4] C. P. Bosman Barros, H. Butler, J. van de Wijdeven, and R. Toth, "On feedforward control of piezoelectric dual-stage actuator systems," in *2021 60th IEEE Conference on Decision and Control (CDC)*, Dec. 2021, no. Cdc, pp. 5588–5594, doi: 10.1109/CDC45484.2021.9683598.
- [5] R. G. C. de Bruijn, J. J. M. van de Wijdeven, and J. P. M. B. Vermeulen, "Enabling piezoelectric wafer stages with highly variable stiffness device for next-generation semicon equipment," in *DSPE Conference on Precision Mechatronics*, September 26-27, 2023.
- [6] J. A.L. de Goeij, R. G. C. de Bruijn, J. P. M. B. Vermeulen, R. W. A. H. Leenaars, and B. Jansen, "Lithographic apparatus stage coupling," Patent WO2023078788A1, May 11, 2023.
- [7] R. Lakes, *Viscoelastic Materials*, vol. 262. Cambridge University Press, 2009.